Technical Report

TR-99-37

Change in coastal sedimentation conditions due to positive shore displacement in Öregrundsgrepen

Lars Brydsten

Department of Ecology and Environment Science
Umeå University

Februari 2000

Svensk Kärnbränslehantering AB
Swedish Nuclear Fuel
and Waste Management Co
Box 5864
SE-102 40 Stockholm Sweden
Tel 08-459 84 00
+46 8 459 84 00
Fax 08-661 57 19
+46 8 661 57 19

Change in coastal sedimentation conditions due to positive shore displacement in Öregrundsgrepen

Lars Brydsten

Department of Ecology and Environmental Science
Umeå University

December 1999

Keywords: waves, resuspension, shore displacement, modelling, SFR, biosphere, SAFE

Sammanfattning

Denna rapport är en del av SKB-projektet "SAFE" (Safety Assessment of the Final Repository of Radioactive Operational Waste). Syftet med SAFE-projektet är att uppdatera den tidigare utförda säkerhetsanalysen av SFR-1. Analysen skall presenteras för svenska myndigheter senast år 2000. SFR-1 är ett förvar för låg- eller medelaktivt radioaktivt avfall beläget i berggrunden under Bottenhavet ca 1 km utanför kusten nära Forsmarks kärnkraftverk i Norra Uppland.

Om radionuklider idag av någon anledning skulle transporteras ut till berggrunden i anslutning till SFR-1, skulle förmodligen den vidare transporten ske med uppåtgående grundvattenströmmar till havsbotten. Många radionuklider har en förmåga att adsorberas till finkorniga partiklar, varför det är troligt att denna adsorbering skulle ske på partiklar i bottensedimentet eller partiklar suspenderade i havsvattnet. Adsorptionen är stark varför den fortsatta transporten av radionukliderna i stor utsträckning skulle styras av dynamiken för de finkorniga partiklarna.

En matematisk modell har konstruerats som simulerar resuspension av finkorniga partiklar orsakade av vågrörelser. Modellen utgår från havsbassängens morfometri och en given vädersituation. Först beräknas vågens egenskaper på djupt vatten (våghöjd, våglängd och riktning) varefter den successiva förändring i vågens egenskaper som orsakas av uppgrundning beräknas. Längs hela vågens färdväg beräknas den maximala orbitala vattenhastigheten vid botten och med hjälp av kända semiempiriska samband avgörs om vågen förmår resuspendera finkorniga partiklar. Ett mycket stort antal vädersituationer simuleras och resultatet utgörs av en karta med två olika bottentyper; accumulationsbotten (kontinuerlig accumulation av finkorniga partiklar och eventuellt även radionuklider) eller transport/erosionsbotten (perioder med accumulation växlat med perioder med erosion). Modellen har kalibrerats mot fyra lokaler i närheten av SFR-1, som sinsemellan har olika sedimentationsförhållanden.

Eftersom strandförskjutningen i området är positiv, f n cirka 60 cm per hundra år (Påsse, 1997), har och kommer sedimentationsförhållandena att ändras över tiden; områden med accumulationsbottnar kan övergå till transportbottnar och vice versa. Det har därför varit nödvändigt att simulera både tidigare och framtida förhållanden genom att manipulera vattenståndet i havet.

Resultatet av simuleringarna visar att sedimentationsförhållandena ändras snabbt men vanligen efter ett tydligt mönster; vid tiden för inlandsisens avsmältning bestod hela området av accumulationsbottnar, allt eftersom uppgrundningen skedde övergick högre partier till transportbottnar (som mest till ca 14 % 500 AD), där vissa av dessa områden senare pånytt övergick till accumulationsbottnar orsakat av den växande skärgårdens skydd mot det öppna havets vågor. Vissa djupt liggande områden, t.ex. djupränna väster om Gräsö, har under hela den postglaciala tiden haft accumulativa förhållanden.

Stora delar av området i anslutning till SFR-1 har nyligen övergått från transportbotten till accumulationsbotten och den trenden fortsätter samt kommer att bestå ända till området blir land (2 400–3 500 AD). Det innebär att om ett utsläpp av radionuklider skulle ske idag finns förutsättningar för att delar av detta utsläpp skulle bindas i bottensedimenten i närområdet till SFR-1, delar bindas i Gräsörännans bottensediment och förmodligen till vissa delar spridas ut över djuphavet. Eftersom andelen accumulationsbotten ökar med tiden innebär det att förutsättningarna ökar för en allt större andel

radionuklider som binds i närområdets bottensediment. Allt eftersom närområdet till SFR-1 blir land kommer det att bildas flera små sjöar och ca 5000 AD en stor sjö ca 2 km nordväst om SFR-1 (Brydsten, 1999). Förhållandena ändras nu dramatiskt då grundvattenströmmarna kommer att mynna i ett utströmningsområde på land eller i botten av en sjö. Förutsättningarna ökar nu för en ytterligare minskad spridning då radionukliderna kan bindas till organiskt material i utströmningsområdena eller till sjöars bottensediment. Den övergripande trenden är att den största spridningen skulle ske om utsläppet skedde idag och successivt mindre spridning med tiden samt en mycket lokal spridningsbild om utsläppet sker efter 5000 AD.

Abstract

This report is a part the SKB project "SAFE" (Safety Assessment of the Final Repository of Radioactive Operational Waste). The aim of project SAFE is to update the previous safety analysis of SFR-1. The analysis is to be presented to the Swedish authorities no later than the end of the year 2000. SFR-1 is a low and intermediate level radioactive waste disposal facility, which is situated in bedrock beneath the Baltic Sea, 1 km off the coast near the Forsmark Nuclear Power Plant in Northern Uppland.

At a possible discharge of radionuclides from SFR-1 today, ground water currents will presumably transport the radionuclides to the sea bottom. Many radionuclides are able to absorb on to fine particles, and it is likely that the radionuclides would adsorb on to particles in the sediment or particles suspended in the seawater. The adsorption is strong, and therefore the dynamics of the radionuclides are governed by the dynamics of the fine particles.

A mathematical model has been developed to simulate the resuspension of fine particles cased by wave movement. The model simulates the wave-induced near bottom water dynamics based on meteorological data. First, the wave's characteristics in deep water are calculated (wave height, length, and direction). Then the gradual change of the wave's characteristics is calculated as it reaches shallower water. The maximum near-bottom orbital velocity is calculated for the entire fetch distance, and the wave's ability to resuspend fine-grained particles is determined using well-known semiemperical methods. A large variety of weather conditions are simulated and the results are shown as a map for two different bottom types: accumulated bottoms (continual accumulation of fine-grained particles and any radionuclides present) and erosional/accumulation bottoms (periods with accumulation alternating with periods with erosion). The model has been calibrated for four areas close to SFR-1, which provides a range of different sedimentation conditions.

Since shore displacement is positive, currently approximately 60 cm per century (Påsse, 1997), sedimentation conditions have fluctuated and will continue to fluctuate over time. Areas with accumulation bottoms can switch to erosional bottoms and vice versa. For this reason, it has been necessary to simulate both previous and future conditions by adjusting the water depth conditions in the sea.

The results of the simulations show that sedimentation conditions change quickly, but normally a clear pattern is evident. At the time the most recent glacial melted away from the region, the entire area was made up of accumulation bottoms. As the land rose and the area became more shallow, many of the bottoms became more erosional (at maximum approximately 14% 500 AD). Certain of these areas later went back to being accumulation bottoms as a result of the growing archipelago which provided protection from the waves of the open sea. Certain deep areas, such as the channel west of Gräsö, have had accumulation conditions for the entire post-glacial period.

Large parts of the area close to SFR-1 have recently shifted from erosional bottoms to accumulation bottoms. This trend is continuing and will continue until the area becomes land (2,400–3,500 AD). This means that should a release of radionuclides occur today, they could in part adsorb on bottom sediment near SFR-1, in part adsorb on bottom sediment in the Gräsö channel and spread to some extent into the deeper waters of the sea. Since the number of accumulation bottoms continually increases, the conditions

improve for an every increasing amount of radionuclides adsorbing on bottom sediment close to SFR-1. As the area around SFR-1 rises to become land, a large number of small lakes will form and a large lake will form approximately 5,000 AD about 2 km north-east of SFR-1 (Brydsten, 1999). After this point the conditions will change dramatically as the groundwater currents will flow into a drainage area on land or at the bottom of a lake. The ability of the radionuclides to spread will continue to decline since they will increasingly be able to adsorb to organic material in the drainage areas or on lake bottom sediment. It is clear that the greatest spread of radionuclides would occur if the release were to take place today. As time goes on, the ability of the radionuclides to spread would gradually decrease. After 5000 AD only very local spreading would occur.

Content

1 Introduction

This report is a part the SKB project "SAFE" (Safety Assessment of the Final Repository of Radioactive Operational Waste). The aim of project SAFE is to update the previous safety analysis of SFR-1. The analysis is to be presented to the Swedish authorities not later than the end of 2000. SFR-1 is a low and intermediate level radioactive waste disposal facility, which is situated in bedrock beneath the Baltic Sea, 1 km off the coast near the Forsmark Nuclear Power Plant in Northern Uppland.

The Gulf of Bothnia is characterised by low wave energies, no tides, low salinity and strong positive shore displacement. The highest shoreline is situated at approximately 270 meters above the present sea level. This means that littoral processes have effected an extensive area around the gulf, and consequently the soil distribution has a clear littoral footprint. On top of the hills the till has been washed away and the rock is visible, on the slopes there is wave-washed till, and fine-grained sediment is found in lower parts of the terrain and in areas sheltered from the sea.

A comparison between the distribution of fine-grained sediment above and below the present sea level shows a more extensive distribution in the littoral zone and even more extensive distribution in deeper parts of the sea. It is obvious that some of the fine-grained sediment in the littoral zone is resuspended and transported to deeper parts of the sea.

The aim of this study is to develop a method for deciding through the use of a mathematical model which fine-grained sediments in the littoral zone will "survive" the littoral processes and which form terrestrial fine-grained post-glacial soils due to positive shore displacement. The model simulates the wave-induced near bottom water dynamics based on meteorological data and the bathymetry of the study area.

The study is being performed because many radionuclides have a capacity to adsorb on fine-grained particles. At a possible discharge of radionuclides from SFR-1 today, ground water currents will presumably transport the radionuclides to the sea bottom. The radionuclides can be adsorbed in the seawater on fine-grained particles. The associations are often strong and therefore the dynamics of the radionuclides are governed by the dynamics of the fine-grained particles. Consequently, it is of great importance to know the sediment dynamics in the coastal area in order to predict the distribution of the radionuclides.

2 Method

Resuspension of fine-grained particles is in most aquatic environments governed by different types of processes, i.e. longshore currents, tidal currents, wind-induced currents and wave orbital motions. In near-shore shallow areas the processes associated with breaking waves are predominant, while in deeper situated bottoms the wave orbital motions are the predominating resuspension processes. In order to decide if resuspension occurs, it is necessary to calculate both the distribution of the maximum grain size, which can be resuspended due to the breaking waves, and the wave orbital motion.

When the water velocity over a bed is increased, eventually a stage is reached when the particles are moved from the bed. The stage is known as the threshold of sediment movement. Many equations have been proposed for determining the threshold of sediment movement due to wave action. In a review by Komar and Miller (1973) it was found that for grain diameters less than 0.5 mm, the threshold is best related by the equation

$$\frac{\rho u_t^2}{(\rho_s - \rho)gD} = 0.21\sqrt{\frac{d_0}{D}} \qquad (1)$$

Where u is the near-bottom threshold velocity, d_0 is the near-bottom orbital diameter, p is the water density, p_s is the density of sediment grains and D is the diameter of the sediment grains.

For grain diameters larger then 0.5 mm, the threshold is best related by the equation

$$\frac{\rho u_t^2}{(\rho_s - \rho)gD} = 0.46\pi\left(\frac{d_0}{D}\right)^{1/4} \qquad (2)$$

Komar and Miller (1975) were able to compare the threshold under waves with the threshold under unidirectional steady currents and found that the equations for waves could also be used for unidirectional currents. Therefore, equation (1) and (2) could also be used for longshore currents generated by the breaking wave.

The grain size of the resuspended material is determinable, provided that the threshold velocity and the orbital diameter are known. These two parameters can be calculated using linear wave theory (Airy, 1845). The horizontal component of the orbital velocity is given by

$$u = \pi H \cosh(k(z-h))\frac{\cos(kx - \sigma t)}{T\sinh(kh)} \qquad (3)$$

where H is the wave height, ó is the wave number (2π/L), L is the wave length, z is the vertical distance to still water surface, positive upward, h is the still water depth, x is the horizontal space co-ordinate, T is the wave period and k is the wave angular velocity (2π/T).

When determining the resuspension of fine-grained sediments due to wave action, the threshold velocity is substituted by the near bottom horizontal component of the orbital velocity. Linear theory assumes waves of small amplitude in deep water, so that it does not accurately describe the water particle motion at shoal depths. Nevertheless, it has been shown experimentally that the linear theory gives a good estimation of the near-bottom horizontal component of the orbital velocity (Le Mehauté et.al., 1968). Furthermore, May and Thanner (1973) found that if the mean value of the horizontal component of the orbital velocity is calculated with Stoke's theory (Wigel and Jonsson, 1951), cnoidal theory (Wigel, 1960) and linear theory (Airy, 1845), the value obtained by linear theory falls between the two others, which both are supposed to better describe conditions at shoal depths.

The near-bottom horizontal component of wave orbital velocity is given by setting Z = -h in equation (3):

$$u_b = \pi H \frac{\cos(kx - \sigma t)}{T \sinh(kh)} \qquad (4)$$

where u_b is the near-bottom horizontal component of wave orbital velocity.

The maximal near-bottom horizontal component of the wave orbital velocity (u_{max}) occurs when cos(kx-σt) = 1 in equation (3), so u_{max} is given by the equation

$$u_{\max} = \frac{\pi H}{T \sinh(kh)} \qquad (5)$$

Airy (1845) gives the near-bottom orbital diameter of the wave motion (d_0):

$$d_0 = \frac{H}{\sinh(2\pi h / L)} \qquad (6)$$

If wave height, wave period and water depth are known, it is possible to calculate the threshold velocity and the near-bottom orbital diameter with equation (5) and (6). Subsequently the maximum resuspendable grain size is determined with equation (1) or (2).

The deep-water wave height and period are predicted using semiempirical methods from known storm conditions, i.e. wind velocity, fetch distance and storm duration. From known wind data the significant wave heights are calculated using the equation (Silvester, 1979).

$$H_{1/3} = \frac{2U^2 \sqrt{\frac{\alpha}{\beta}}}{g} \qquad (7)$$

$$\alpha = 0.0081 \left(\frac{F}{F_{FAS}} \right)^{-0.194} \qquad (8)$$

$$\beta = 0.1 e^{\left[(\ln 7.4)(\frac{F}{F_{FAS}})^{-0.284} \right]} \qquad (9)$$

$$\frac{F}{F_{FAS}} = \frac{F}{16U^{1.5}} \qquad (10)$$

where $H_{1/3}$ is the significant wave height, U is the wind speed, g is the acceleration of gravity, F is the fetch and F_{FAS} is the minimum fetch for fully arisen sea.

The wave period is calculated using the equation

$$T = \frac{2\pi U}{g}\left(\frac{3}{4}\right)^{0.25} \qquad (11)$$

As the waves enter shallow water they undergo a transformation. The wave velocity and length decrease progressively, the height increases but the period remains constant.

A mathematical model for determining this transformation is presented in May (1974). The model is based on linear theory and calculates the transformation caused by shoaling, refraction and bottom friction. The wave is approximated to a number of wave rays, i.e. lines drawn normal to the wave crest in the direction of wave advance. The computer program tracks the wave rays from deep water to the shore. The wave direction and phase velocities are recalculated at short intervals along the rays. The change in wave height is computed using the following equation (May, 1974):

$$H_i = H_0\left(K_r \frac{\cosh^2 kh}{0.5\sinh(2kh+kh)}\right)^{1/2} - 0.67\left(\sum_{j=1}^{i}(x_j - x_{j+1})\left(\frac{Tc_f\sigma^3 H^2}{L\pi g \sinh^3(k_j d_j)}\right)\right) \qquad (12)$$

where subscript 0 refers to deep water, i to point in shoal water and j is the jth increment along the path of the wave ray. The refraction coefficient (K_r) is calculated by reference to equal points in time on adjacent rays. The friction coefficient (C_f) is empirically determined to 0.03 (May and Tanner, 1973).

If the ray reaches shore, the point where the wave is breaking is determined using solitary theory by the equation

$$\gamma_b = \frac{H_b}{h_b} = 0.78 \qquad (13)$$

The longshore current velocity is calculated with radiation stress approach using the equation (Komar, 1975)

$$v_l = 2.7u_{\max}\sin\alpha_b\cos\alpha_b \qquad (14)$$

where α_b is the angle between the wave crest length and a line parallel to the shoreline.

The maximal resuspendable grain size due to the longshore current is then calculated with equation (2).

3 The computer program

The program consists of two parts, one for simulation and one to handle the results.

The simulation program is written in C++ (1100 rows of code) and requires the following inputs:

– Depth values in a regular grid (xy matrix) with values at point of intersection. Depth values and related co-ordinates from both the shore and the sea are needed. Altitude values for the shore can be found in digital topographic maps, digital altitude grids or by digitising topographical paper maps. Depth values can be captured from digital charts or by digitising paper charts. If the captured data is of line type, the lines must be transformed to points using GIS. The irregularly spaced points are transformed to a regular grid using a method based on Kriging interpolation (Davis, 1986).

– Meteorological data. The wind speed, duration and direction at the upwind part of the basin are required.

With this information the computer program tracks wave rays from deep water to the shore. The maximal horizontal component of the orbital velocity and the maximal resuspendable grain size are calculated at short intervals along the ray. If the wave breaks in shallow water, the longshore current velocity and direction are calculated. The maximal resuspendable grain-size due to the longshore current is also calculated. By repeating the program with new starting co-ordinates at short intervals along the wave crest, it is possible to calculate the distribution of maximal resuspendable grain-size over the study area.

The wave refraction causes different spacing of calculation points over the study area. In areas with diverging wave rays, it is necessary to simulate wave rays at closer intervals along the wave crest. However, this can lead to a superfluity of results being generated for the deeper parts of such areas. Therefore a database for handling the results is linked to the simulation program. The study area is divided into quadratic cells, where the dimension of the cells depends of the level of detail desired. Only one record is stored for each cell in the result database. The record contains the following parameters:

- X co-ordinate – the east-west co-ordinate in RT90 (the Swedish national grid) of the centre of the cell
  Y co-ordinate – the north-south co-ordinate
- MaxOrb – the maximum near-bottom orbital velocity within the cell
- MaxSize – the maximum resuspendable grain size within the cell
- N – the total number of calculated values within the cell
- SumSize – the sum of all calculated MaxSize
- SumSqSize – the sum of all squared MaxSize

The database is updated for each calculated maximum resuspendable grain-size. If the new calculated MaxSize or MaxBreakSize is greater than the value in the database, the new value is stored in the result database. The items N, SumSize and SumSqSize are updated and are used for calculation of the average size (AvSize) and variance in MaxSize within each cell (VarSize).

4 Model calibration

The model is calibrated on and applied to the coastal area close to SFR-1 (Figure 1). The outer model area is marked with a rectangle in the figure, while the inner model area (marked with a red line in the figure) is defined as the watershed to a future lake which will be formed approximately 5,000 AD (Brydsten, 1999). The model areas are the same for all sub-projects within the SAFE-project, where some models are only applied to the inner model area, while other models (i.e. this sub-project) are applied to the outer model area.

The outer model area is impressed by glacial and littoral processes. The dominating soil is a boulder rich till deposited by a northerly ice flow. The glacial ice melted off the area approximately 9,500 BP and the sea level was at least 50 meters above the present sea level. This means that all the land within the model area has been affected by wave washing. In areas with the strongest wave washing, the till soil is completely removed and the bedrock is visible. In areas with weaker wave washing, the till is eroded from the fine-grained fraction. This fine-grained fraction has often redeposited as post-glacial sediment in lakes or deeper parts of the coastal area where it often overlay glacial clay.

The coastal area is shallow and rich in islands. The deepest part is a north-south channel on the west side of Gräsö (Figure 1). The area is relatively exposed to the north so the sediment dynamics are influence by the waves generated in the Bothnian Sea. The area is also in contact with the Baltic Proper through a narrow sound, Öregrundssundet. The sound is so narrow that waves generated in the Baltic Proper cannot affect the sediment dynamics within the model area.

The model is calibrated to four areas with different geological conditions:

Site 1. The bottom above SFR-1 with a total lack of post-glacial fine-grained sediment (Sigurdsson, 1987).

Site 2. A number of soil samples taken north and north-east of SFR-1 in an area with small patches of post-glacial fine-grained sediments (Kautsky, 1999).

Site 3. A shoal bay close to SFR-1 with thin layers of post-glacial, organic rich fine-grained sediment (Wallström et al, 1997).

Site 4. An accumulation bottom in the deep channel west of Gräsö with thick layers of post-glacial fine-grained sediments (Notter, 1988).

The Swedish Geological Survey has carried out a sea bottom survey in an area above SFR-1 (Site 1 in Figure 1) (Sigurdsson, 1987). The survey was done with common marine geophysical instruments and sediment sampling with what is referred to as a “till sampler”. The results show a bottom dominated by wave-washed till and small areas with glacial clay, i.e. a total lack of post-glacial fine-grained sediments.

Five sediment samples were taken north of SFR-1 in the deepest part of the region (Site 2 in Figure 1) (Kautsky, 1999). The bottom is characterised by large boulders with sandy sediments between but in some places patches of silty sediments. This means that the area today has an accumulation environment for silt particles but the lack of widely spread sediment areas indicates that the sedimentation period has been short.

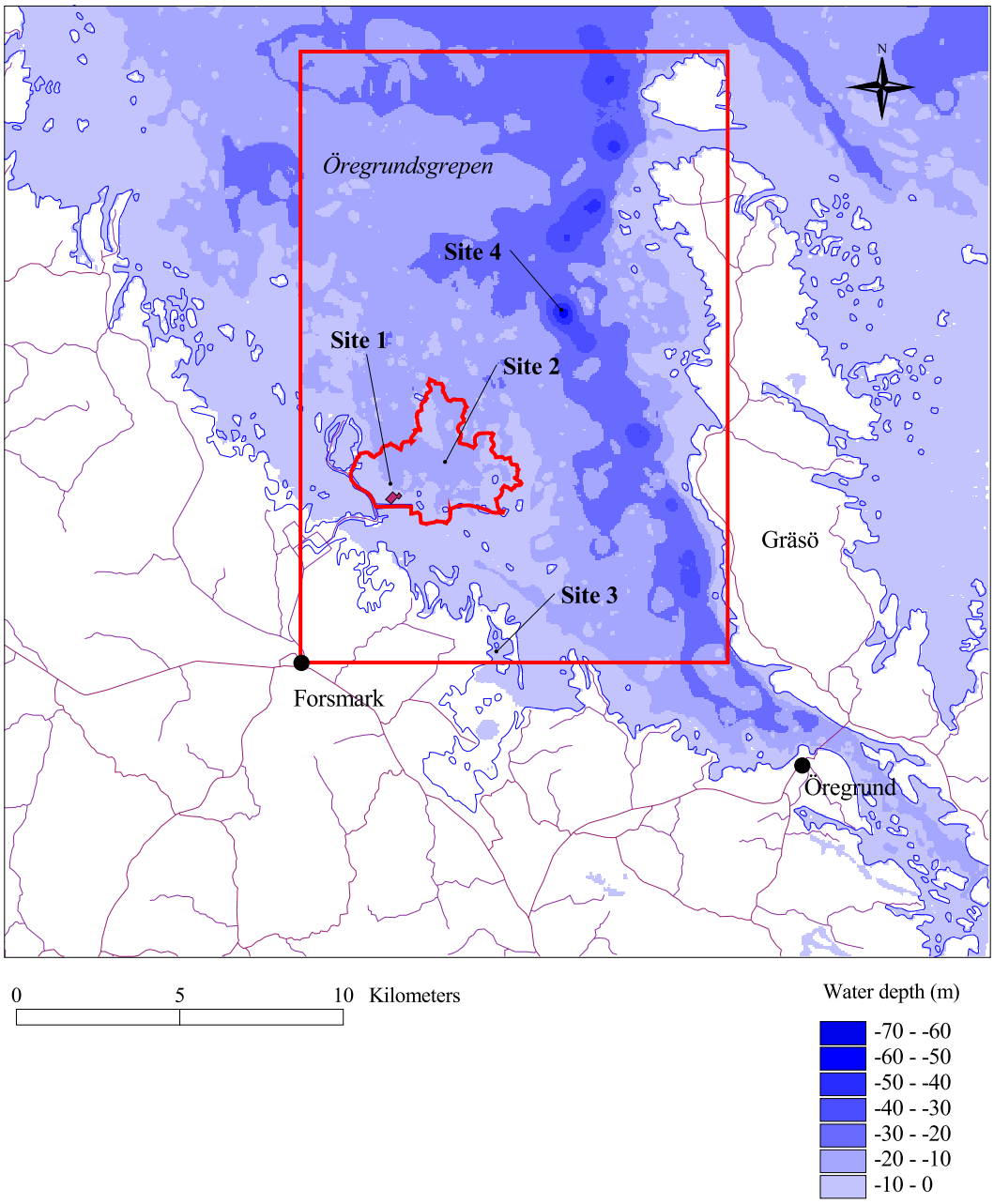

Figure 1. *The study area with the outer model area marked with a rectangle, the inner model area with a red line and the possitions of the four calibration sites. Permission: The National Land Survey of Sweden.*

Some shoal sea bays in the western part of Öregrundsgrepen have been investigated concerning sediments (Wallström et al, 1997). One bay close to SFR-1, Kallrigafjärden (Site 3 in Figure 1), has a bottom dominated by fine-grained, organic rich sediments.

According to Notter (1988), there are accumulation bottoms in the deep channel on the west side of Gräsö with thick layers of post-glacial fine-grained sediments. The thickness proves that sedimentation has occurred for a long period. The two deepest basins are selected as calibration areas (Site 4 in Figure 1).

Altogether, four areas are selected for calibration: one area with accumulation over a long period, one with a limited accumulation period, one that recently switched from erosional to accumulation environment and one area with a total lack of post-glacial fine-grained sediments, i.e. an erosional environment. The change of maximum resuspendable grain size (MRGS) over time will be simulated for these areas, and both the trend and present level of MRGS will be used to distinguish between areas with erosion and accumulation of fine-grained particles.

4.1 The resuspension model

The resuspension model is run for every combination of:

- wind speeds between 5 and 25 m s^{-1} with 1 m s^{-1} steps,
- wind directions from 170 to 250 degrees in 10 degree steps,
- sea water level for the period –6,000 AD to 3,000 AD in 500 year steps (73 meters above present sea level to 6 meters below present sea level).

Approximately 10,000 simulations were performed.

The reason for simulating different wind speeds instead of only the highest wind speed recorded is that the program uses only the significant wave height while in nature the wave train also contains waves with lower heights. A high and steep wave can break in deep water or break when passing a shallow part of the basin, while lower and steep waves can reach the shore. Thus, the highest wave energies close to the shore are not necessarily due to waves generated by the highest wind speeds, and consequently it is necessary to simulate a range of wind speeds.

The resuspension model generated a grid with MRGS values in Arc/Info Ascii Grid format. The grid was imported to ArcView. The four calibration sites were digitised on screen to ArcView shape format. The grid cells within each calibration site were selected using an Avenue script in ArcView. The average value and the standard deviation were calculated for the selected MRGS values for each time step.

Figure 2 shows the change in MRGS over time for the SFR-1 site (Site 1 with erosional environment). The time development is typical for a site with an open slope, i.e. a slope that is affected by breaking waves, in contrast to a closed slope that is a part of a local basin and that will become a lake bottom. When the water depth is high, the MRGS is low or zero, but as the water depth decreases the MRGS increases, known as the shoaling effect. As the water level decreases, the effect of breaking waves in the coastal area increases, and only waves with lower energy will reach the shore, known as the energy filter effect. In the early part of the process, the shoaling effect is the dominating effect, but in the Öregrundsgrepen area the energy filtering effect becomes the dominating effect after approximately 3000 BP. The last stage in the time development is a rapidly increased MRGS. This is due to water dynamics associated with breaking waves and is therefore only found in low water depths.

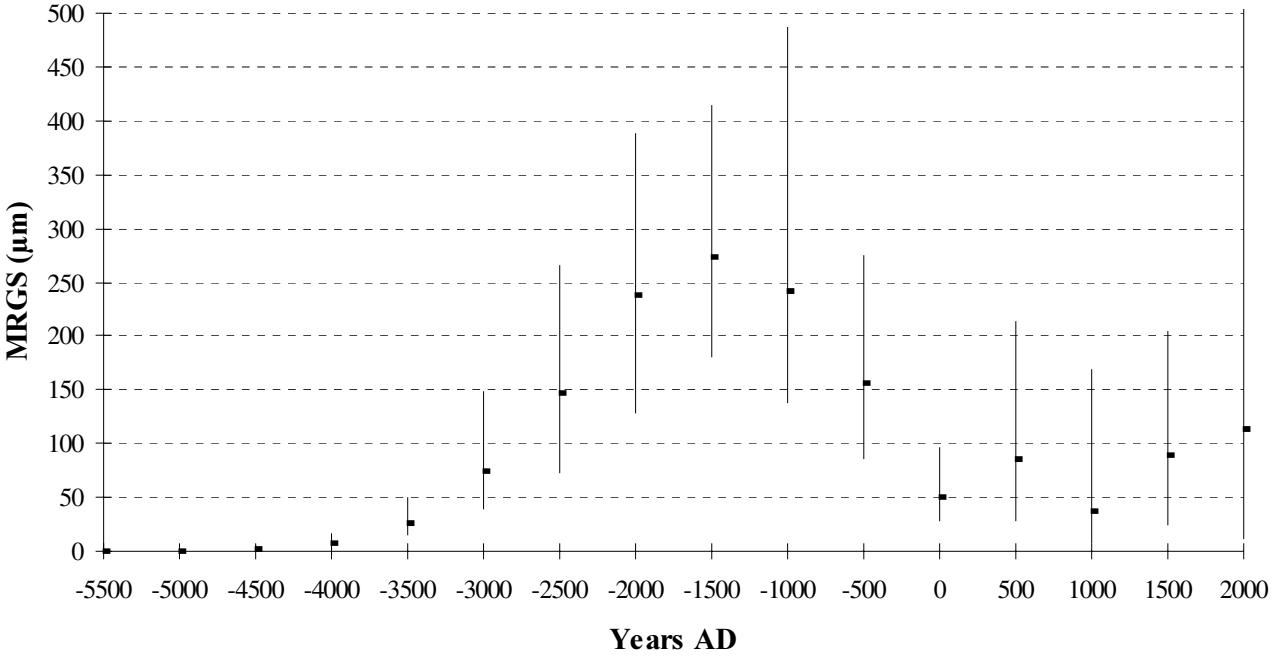

Figure 2. *The change in MRGS over time for the SFR-1 site (Site 1). The stock diagram shows the average value and +/- one standard deviation.*

As noted earlier, the SFR-1 area (Site 1) lacks post-glacial, fine-grained particles. After the inland ice melted off (–7000 AD), the area was an accumulation environment for at least 3,000 years. This period was followed by a long period with an erosional environment, presumably up until today. It is possible that it was an accumulation environment during the period with low MRGS between 0 and 1,000 AD, with sediments that later could have been eroded during the wave breaking stage. Nevertheless, the figure shows that the dividing MRGS must be lower than 100 µm.

Figure 3 shows the MRGS-values for the deep area north of SFR-1 (Site 2 with 19 meters water depth). The level of the shoaling peak of MRGS is much lower compared to the SFR-1 site (Site 1), and the wave breaking effect is lacking since the site is located in a local basin. The site has only minor patches of post-glacial fine-grained sediments, which, as previously noted, is an indicator of a recent switch from an erosional to an accumulation stage. The lack of extensive fine-grained sediments at the site indicates an earlier long period with an erosional environment. This means that the dividing MRGS should be lower than approximately 20 µm. This also implies that the fine-grained sediment found at the site is newer than 500 years.

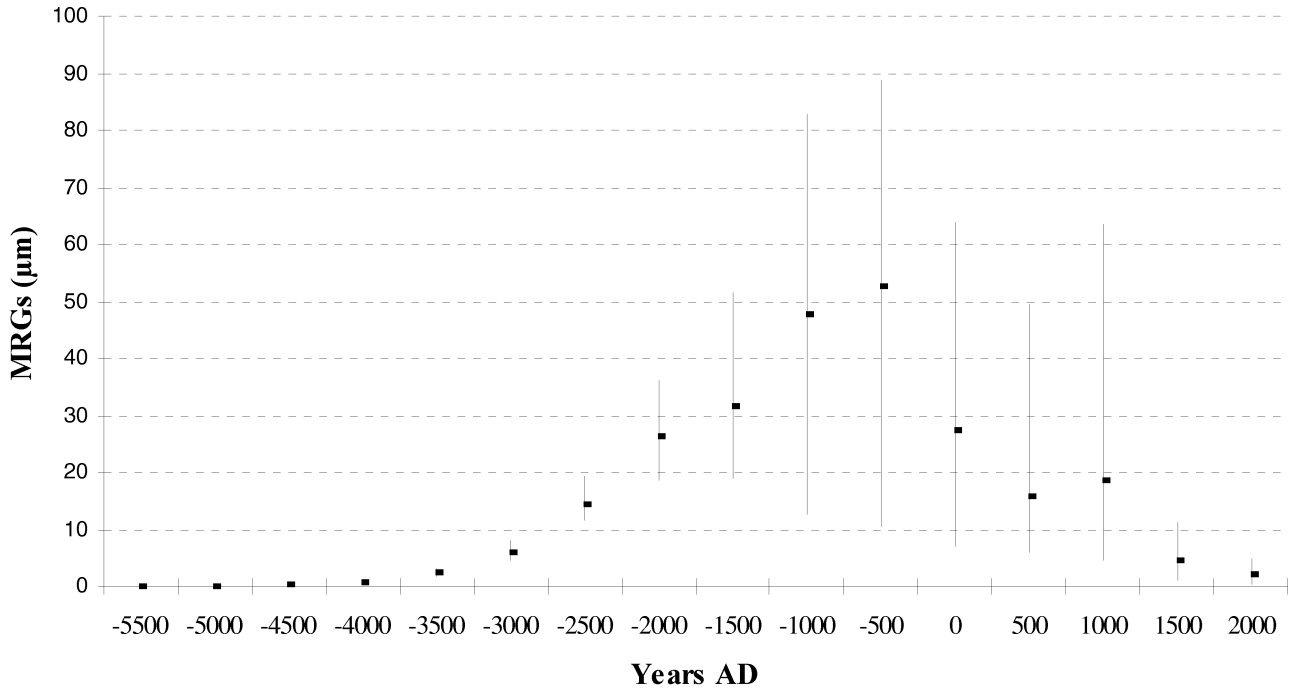

Figure 3. *The change in MRGS over time for site 2. The stock diagram shows the average value and +/- one standard deviation.*

The average values of MGRS from Site 3 are shown in figure 4. It has the same pattern as the Site 2 but the late decrease is earlier, and the time to build up fine-grained sediments was approximately twice as long compared to Site 2. Except for this, the site gives no other facts that help determine the dividing MRGS level.

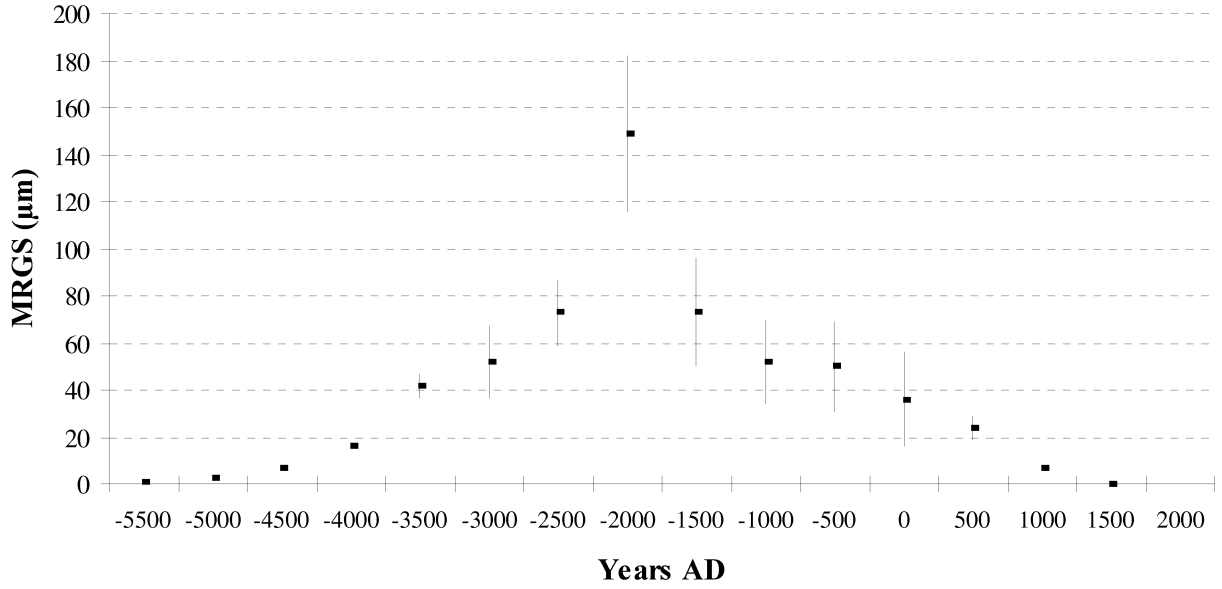

Figure 4. The change in MRGS over time for the Kallrigafjärden (Site 3). The stock diagram shows the average value and +/- one standard deviation.

The results from the site with thick post-glacial fine-grained sediment (Site 4) are shown in figure 5. The presence of thick layers of post-glacial fine-grained sediments at the sites indicates that the area has been in an accumulation stage for the entire period after the glacial ice cover melted off. This means that the dividing MRGS level must be above approximately 15 µm.

Taking all four calibration sites into consideration, the dividing MRGS level is approximately 20 µm. This is also the upper grain size for particles with a high degree of adsorption of radionuclides.

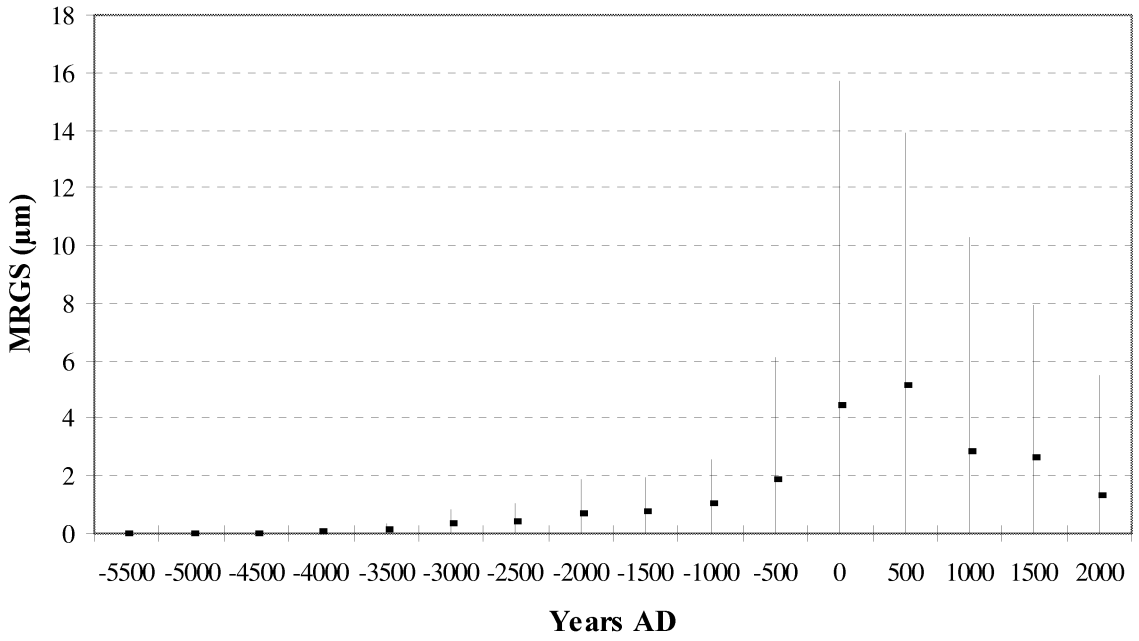

Figure 5. *The change in MRGS over time for the Gräsö Channel (Site 4). The stock diagram shows the average value and +/- one standard deviation.*

5 Results

The model calibration led to the definition of an accumulation bottom as a bottom with a maximum resuspension grain size (MRGS) of less than 20 µm. Erosion bottoms were thus defined as bottoms that the model indicates have a MRGS larger than 20 µm.

The shift between the two types of bottoms over time for both the outer (solid line) and inner model areas (dotted line) is shown in figure 6. The glacial ice cover melted from the area approximately 9500 BP (–7,500 AD) and accumulation bottoms are present throughout the area of study. The shift from accumulative to erosional environments began approximately –5,550 AD. This occurs in the highest areas in the outer model's south-west section. A gradual decrease in the number of accumulation bottoms from 100% down to approximately 14% occurs for the outer model area during the period –5,500 to 500 AD. From this point until the present day, the number of accumulation bottoms increases to approx. 31%, and this increase will continue until approximately 3,000 AD when approximately 43% of bottoms will be accumulation bottoms.

A comparison of the development of the outer and inner model areas over time (Figure 6) shows that the inner model area changed more quickly and was only made up of erosional bottoms during the period –2000 to 500 AD. The explanation for this difference is that the inner model area has a shorter interval in terms of water depth and that a change initiated by a change in water depth influences the entire area for a shorter period.

Figure 6. *The change in % accumulation bottom over time for the outer (solid line) and inner model area (dotted line).*

The extent of the accumulation bottoms at the time they were at a minimum (500 AD) is shown in Figure 7. The larger occurrences are located along the Gräsö Channel, the deep channel that runs north to south parallel with the west coast of Gräsö. The change in the extent of the accumulation bottoms from 500 AD to the present is primarily the result of existing accumulation areas that have grown in size (Figure 8). This trend will continue until at least 3,000 AD (Figure 9).

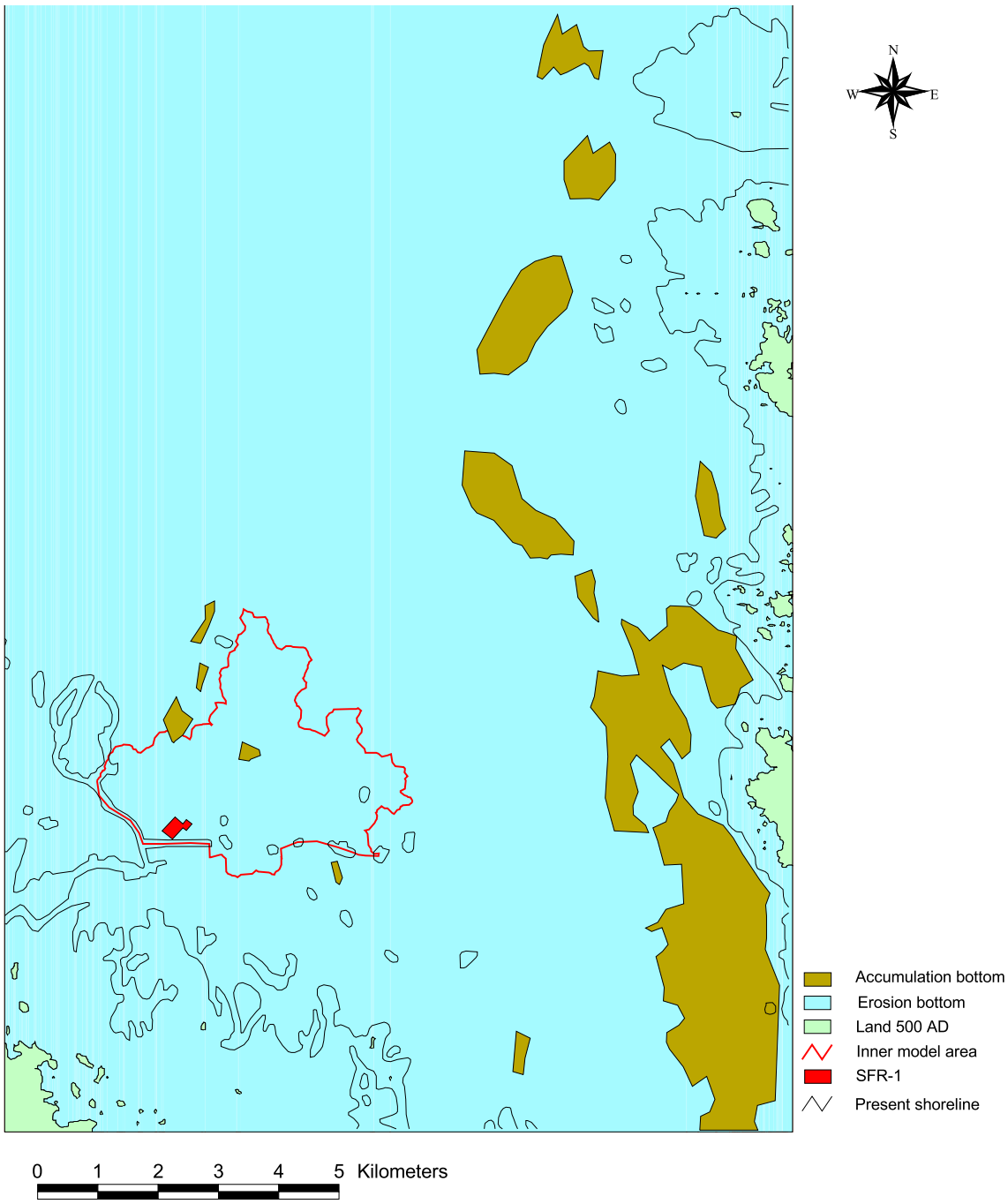

Figure 7. *The extension of accumulation bottoms for the outer model area at 500 AD. The accumulation bottom is defined as bottoms with average MRGS-values lower than 20 µm. The black line is the present shoreline.*

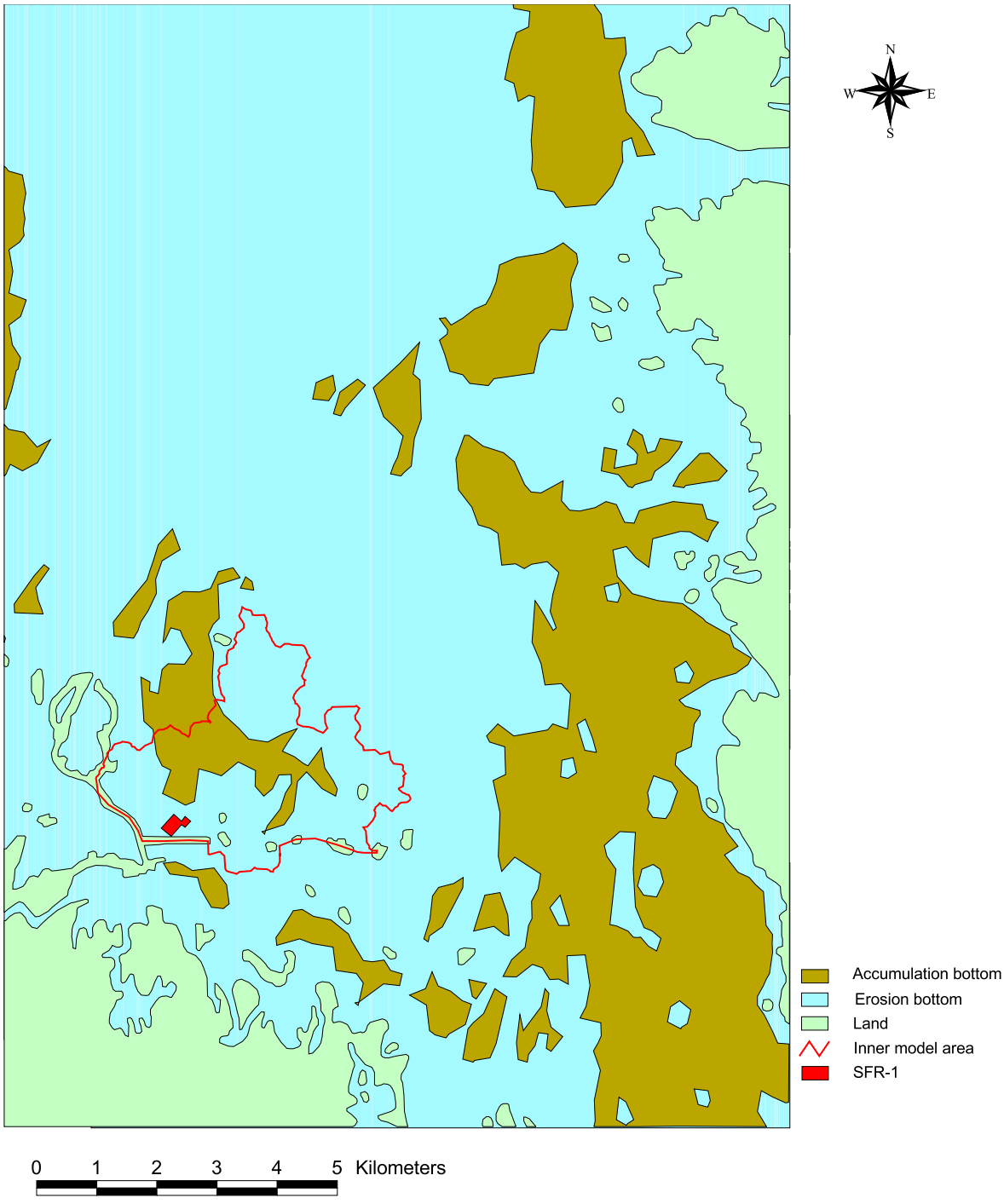

Figure 8. *The extension of accumulation bottoms for the outer model area at present (2000 AD). The accumulation bottom is defined as bottoms with average MRGS-values lower than 20 µm. The black line is the present shoreline. Permission: The National Land Survey of Sweden.*

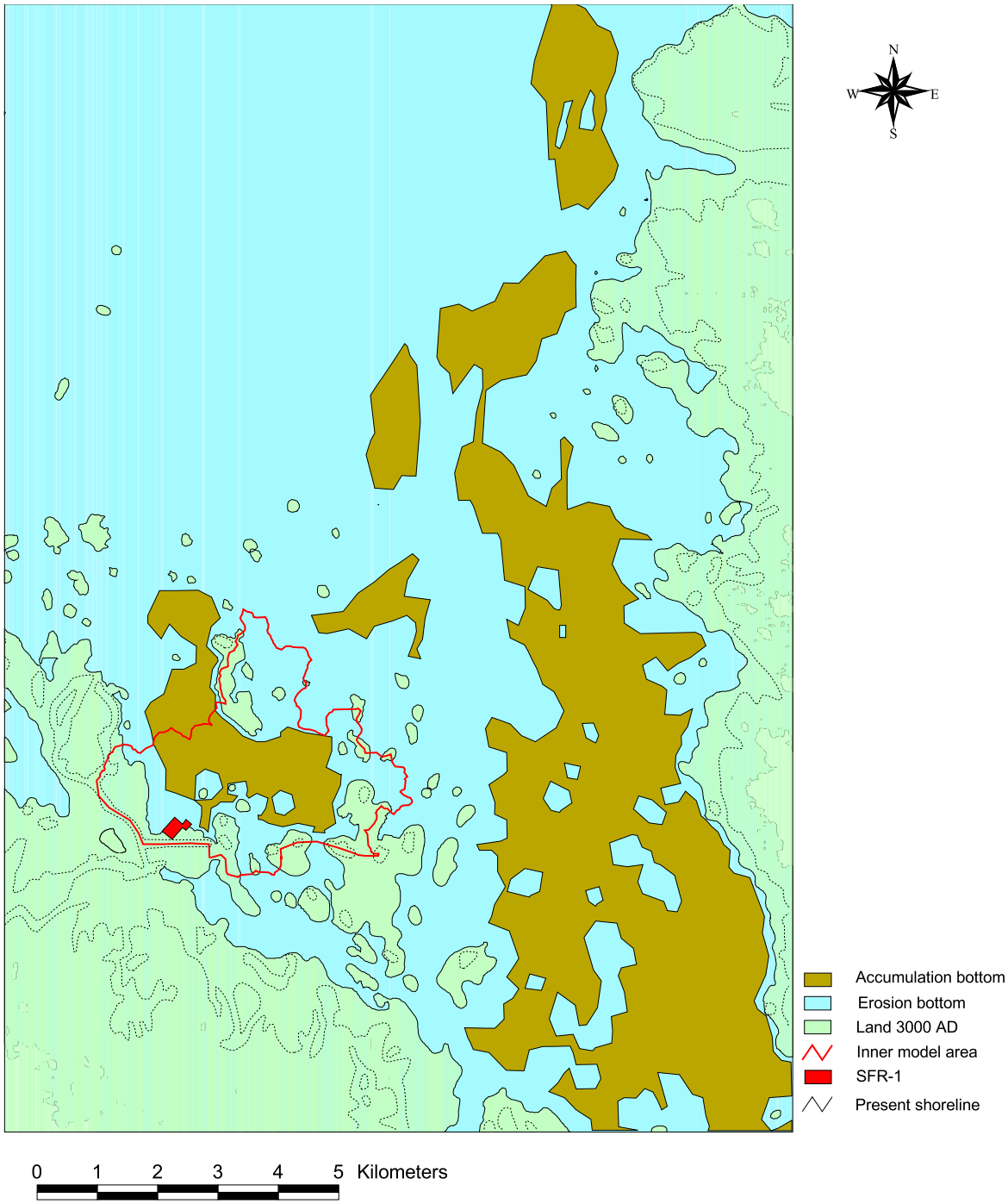

Figure 9. *The extension of accumulation bottoms for the outer model area at 3000 AD. The accumulation bottom is defined as bottoms with average MRGS-values lower than 20 µm. The dotted line is the present shoreline.*

The inner model area, as noted previously, has been influenced by erosion for approximately 2500 years until 500 AD (Figure 6). The first accumulation area after this period developed on the leeward side of a shallow rock outcropping, which protected it from the waves generated in the open sea, and not the deepest sections of the inner model area. The number of accumulation bottoms increased rapidly from 500 AD (0%) to the present (23%), primarily as a result of the increasing shallow areas that developed in the inner model area's northern and north-eastern sections.

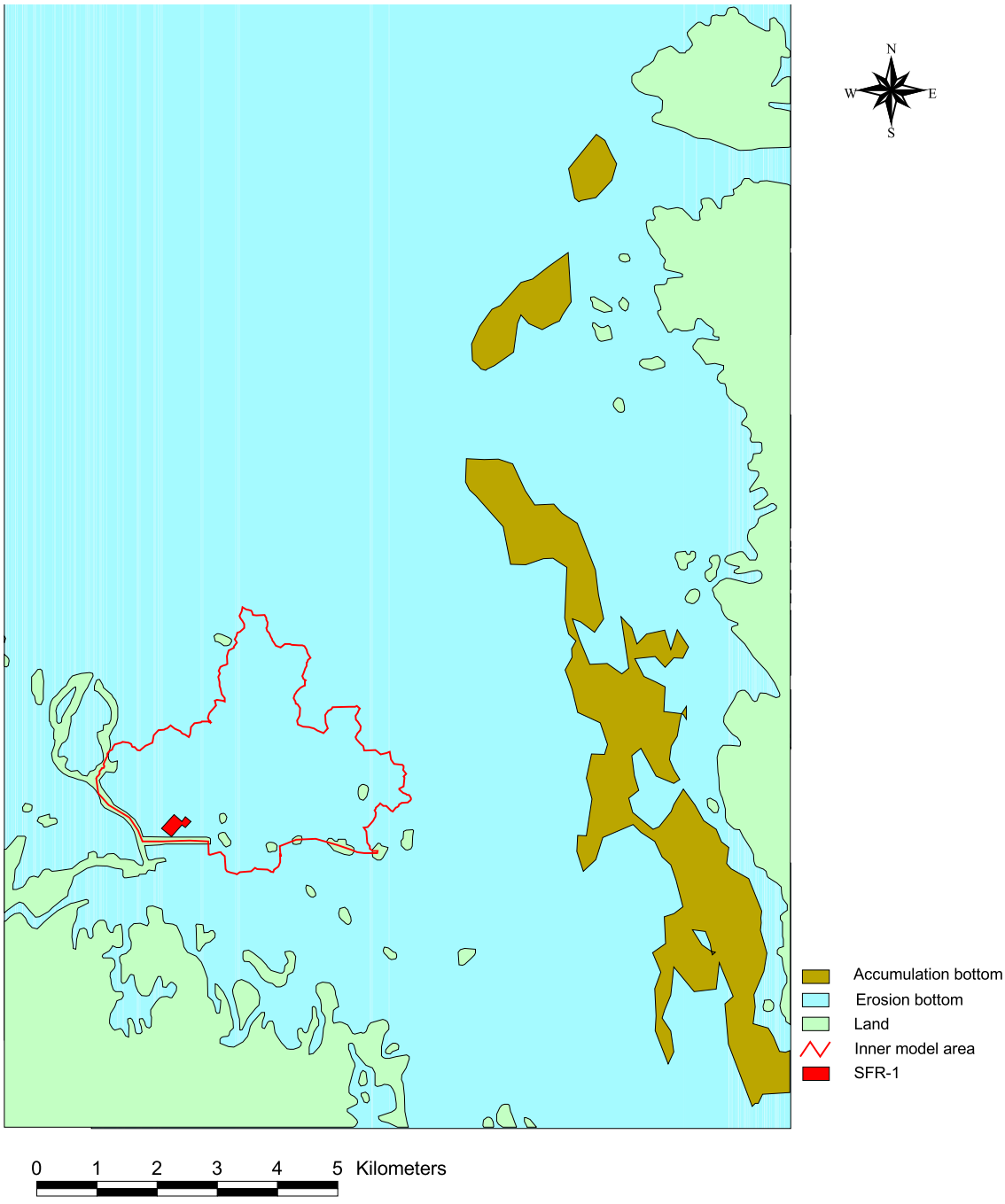

Figure 10. *The extensions of areas that have accumulative environments during the entire period –7500 AD until the present. Permission: The National Land Survey of Sweden.*

Figure 10 shows the areas that have accumulative environments during the entire period –7500 AD until the present. These areas are most likely made up of thick accumulations of fine-grain sediment. The areas correspond with the deep channel west of Gräsö and correspond relatively well with the empirical results presented in Notter (1990) and in Mo and Smith (1988). Note that no such bottoms occur within the inner model area.

6 Discussion

The time development with the increase in the number of accumulation bottoms as illustrated in Figures 7, 8, and 9, with 100% accumulation bottoms after the glacial ice receded, a general decrease in the number for a period followed by an increase to the present is the result of two opposing effects: the shoaling and the wave energy filter effects of the coastal areas.

The shoaling effect is caused by the fact that the water's orbital movement of a wave decreases exponentially with the depth under the water surface. In other words, the shallower the water, the higher the horizontal orbital speed at the bottom and thus an increase in the ability for resuspension. The shoaling effect alone causes gradually lower numbers of accumulation bottoms as the positive shore displacement progresses.

The coast's wave energy filter effect is determined both by the density of the islands in coastal areas and the water depths of the coastal area. Waves with high energy generated in open sea brake on the island shores or when the waves pass shallow areas without breaking. The process results in high wave energies being filtered out while low wave energies are able to pass. Over time, the positive shore displacement results in increased density of islands and shallow areas becoming even shallower thus increasing the filter effect. An increased filter effect results in an increased number of accumulation bottoms.

Figure 6 can therefore be interpreted as the shoaling effect dominating the filtering effect during the period –6,000 AD to 500 AD while the opposite situation occurs during the period 500 AD to the present. The pattern should be general for all island coastal areas with positive shore displacement. The time of the minimum number of accumulation bottoms however and the degree of change of the coastal areas are determined by topography.

A third effect, the wave breaking effect, is illustrated in figure 2. The effect occurs only at bottoms where morphometry results in breaking waves when the depth of water is less than approximately 5 meters. The water movements occurring under a breaking wave are generally much higher than wave-induced near bottom horizontal orbital movements under non-breaking waves. The number of accumulation bottoms therefore decreases again at near-shore shallow bottoms because the wave breaking effect dominates over the filter effect.

The spreading of the current accumulation bottoms in the inner model area as the model predicts (Fig. 8) is much more wide-spread than observations by divers have been able to identify (Kautsky, 1999). One reason for the difference between observed and modelled conditions can be that the shift from erosional and accumulative environments has occurred relatively late. The bottoms have not had time to build up with fine-grain sediment. Another reason could be that the availability of fine-grain particles in the inner model area is limited after such a long period of extensive erosion.

As noted earlier many processes cause erosion in coastal areas, where wave generated orbital water motions and barotrofic currents are the most significant for resuspension of fine-grained particles . The prevailing opinion is that the orbital motion is the most significant resuspension process while the currents are the most important process for the transport of the already suspended particles (Komar, 1976; Gidhagen, 1998).

Within the SAFE project, the current field has been modelled for every third minute during a year as a part of the calculation of water exchange in the model area (Enqvist & Oleg, 1999). The baroclinic model gives the current velocity and direction at approximately 5000 points within the outer model area. In order to compare the significance of wave generated orbital motions with baroclinic currents for resuspension of fine-grained particles; a single storm event has been selected from the baroclinic model result database. The north-easterly storm occur the 11 October 1992 with wind speeds above 25 m s^{-1}, i.e. winds that gave both strong currents and high waves within the model area.

The wave model thus gives the maximum values of the orbital water movement close to the bottom (the average value of the highest 20 values recorded in each cell) for a combination of different wind speeds and wind directions, i.e. the maximum value over a long time. The baroclinic model shows among other things the uni-directional water current fields close to the bottom on this particular occasion. The comparison is therefore not optimal due to the different time spans, but the comparison nevertheless gives a rough measure on the significance of the two processes.

The result database from Enqvist & Oleg was converted from Fld-format to ArcView Shp-format and was integrated in the GIS application for the wave model. The critical water velocity for resuspension of particles with a diameter of 20 µm is approximately 30 cm s^{-1} (Gidhagen, 1998). With this current velocity, the values were classified into accumulation or erosion environment, respectively. The comparison between the sedimentation environment predicted by the wave model (figure 8), and the baroclinic model was made with overlay technique in the GIS application and is presented in Table 1.

Table 1. A comparison between erosion and accumulation environments predicted by the wave model and the baroclinic model, respectively. Values are in % of the total number of points in the baroclinic model result database (5388 points).

		Wave model	
		Erosion	**Accumulation**
Baroclinic model	Erosion	6.7	0.1
	Accumulation	70.3	22.1

It appears from the table that the wave model predicts a much larger extension of erosion bottoms compared to the baroclinic model, 77% and 7% respectively. Empirical studies in the area (Mo & Smith, 1988; Notter, 1990; Persson et al, 1993; Sigurdsson, 1987; Wallström et al,1997) indicate an extension of erosion bottoms larger than 80%. Only 0.1% of erosion bottoms predicted by the baroclinic model are within areas where the wave model predicts accumulation bottoms. The extension of different bottom types predicted by the wave model (e.g. figure 8) would therefore not be changed if the baroclinic processes were added to the wave model.

The ultimate question is how will particle adsorbed radionuclides spread if they are released in the water in the inner model area. Since the relatively large area with accumulation bottoms occurs next to SFR-1, the conditions exist for a part of the particle adsorbed radionuclides to settle in sediment. The contaminated particles, which quickly leave the inner model area with the currents, should settle to a large degree in sediment in accumulation bottoms along the Gräsö Channel and they would to a small degree leave the Öregrundsgrepen and spread in the major currents in the Baltic Sea.

From present to 5,000 AD, the amount of radionuclides which settle in sediment in the inner model area increases since the number of accumulation bottoms are increasing gradually during the period. An important change occurs approximately 3,000 AD when the Öregrundssundet is drained and the Öregrundsgrepen transforms from a sound to a bay (Brydsten 1999). After this point in time, all transports out to the Baltic Sea will have to occur to the north, and the time suspended particles will remain in Öregrundsgrepen should increase. A sedimentation of the bay will likely increase and the likelihood of large scale spreading of radionuclides will decreases.

At approximately 5,000 AD the inner model area will consist of a large lake, till and bogs (Brydsten, 1999). If the release occurs after 5,000 AD, all the contaminated material should either adsorb in organic material or settle as sediment in the lake.

In summary, it can be established that the largest spread would occur if the release occurred today. Gradually, spreading would decrease until 5,000 AD and only a limited spread within the inner model would occur if the release took place after 5,000 AD.

References

Airy, G.B., 1845. Tides and waves. Encyc. Metrop., Art., 192:241–396.

Brydsten, L., 1999. Shore level displacement in Öregrundsgrepen.
SKB TR 99-16, Swedish Nuclear Fuel and Waste Mngt. Co., Stockholm, Sweden.

Davis, J.C., 1986. Statistics and data analysis in geology. John Wiley & sons, New York, p 383–404.

Enqvist, A. & Oleg, A., 1999. Water exchange of Öregrundsgrepen.
SKB, TR-99-11, 59 pp, Swedish Nuclear Fuel and Waste Mngt. Co., Stockholm, Sweden.

ESRI, Environmental systems research institute, 1996. ArcView Spatial Analyst, manual, 147 pp.

Gidhagen, L., 1998. Simulation of deposition and resuspension in the Öre Estuary.
B 165, 1998, Earth Science Centre, Göteborg University, 27 pp.

Kautsky, H., Plantman, P. & Borgiel, M., 1999. Quantitative distribution of aquatic plant and animal communities in the Forsmark- area.
SKB-R-99-69. Swedish Nuclear Fuel and Waste Mngt. Co., Stockholm, Sweden.

Komar, P. D., 1976. Beach processes and sedimentation. Prentice-Hall, London, 429 pp.

Komar, P.D., Miller, M.C., 1973. The threshold of sediment movement under oscillatory water waves. J. Sediment. Petrol., 43:1101–1110.

Komar, P.D., Miller, M.C., 1975. On the comparison between the threshold of sediment motion under waves and unidirectional currents with a discussion of the practical evaluation of the threshold. J. Sediment. Petrol., 45:362–367.

Le Mehauté, B., Divoky, D., Lin, A., 1968. Shallow waves: a comparison of theories and experiments. Proc. 11th Conf. Coastal Eng., p 86–107.

May, J.P., 1974. Wavenrg: A computer program to determine the distribution of energy dissipation in shoaling water waves with examples from coastal Florida. – In: Sediment transport in the nearshore zone. Florida Bureau of Geology. Tallahassee, p 22–79.

May, J.P., Tanner, W.F., 1973. The littoral power gradient and shoreline changes. In: Coastal Geomorphology, ed. D. Coates, Allen & Unwin, London, p 43–60.

Mo, K., Smith, S., 1988. Mjukbottenfaunan i Öregrundsgrepen 1978–1986.
Naturvårdsverket, Rapport 3467, 43 pp.

Notter, M., 1990. Cesium i den marina miljön runt Forsmark efter Tjernobyl.
Naturvårdsverket, Rapport 3723, 14 pp.

Norusis, M., 1993. SPSS for Windows, Advanced statistics, release 6.0, 578 pp.

Persson, J., Wallin, M., Wallström, K., 1993. Kustvatten i Uppsala län 1993. Upplandsstiftelsen, rapport 2, 246 pp.

Sigurdsson, T., 1987. Bottenundersökning av ett område ovanför SFR, Forsmark. SKB, arbetsrapport SFR 87-07, 16 pp.

Silvester, R., 1979. Coastal engineering, I. – Elsevier, Amsterdam, 457 pp.

Wallström, K., Persson, J., 1997. Grunda havsvikar i Uppsala län – Västra Öregrunds–grepen. Upplandsstiftelsen, stencil 12, 47 pp.

Wiegel, R.L., 1960. A presentation of cnoidal wave theory for practical application. J. Fluid Mech., 7:273–286.

Wiegel, R.L., Johnson, J.W., 1951. Elements of wave theory. Proc. First Conf. Coastal Eng., p 5–21.

ISSN 1404-0344

CM Gruppen AB, Bromma, 2000